Diego interacts with Prickle and Strabismus/Van Gogh to localize planar cell polarity complexes

Gishnu Das[1], Andreas Jenny[1], Thomas J. Klein[1], Suzanne Eaton[2] and Marek Mlodzik[1,*]

[1]Brookdale Department of Molecular, Cell and Developmental Biology, Mount Sinai School of Medicine, One Gustave L. Levy Place, New York, NY 10029, USA
[2]Max Planck Institute of Molecular Cell Biology and Genetics, Pfotenhauer Strasse 108, 01307 Dresden, Germany
*Author for correspondence (e-mail: marek.mlodzik@mssm.edu)

Accepted 17 June 2004

Development 131, 4467-4476
Published by The Company of Biologists 2004
doi:10.1242/dev.01317

Summary

Planar cell polarity (PCP) in the *Drosophila* eye is established by the distinct fate specifications of photoreceptors R3 and R4, and is regulated by the Frizzled (Fz)/PCP signaling pathway. Before the PCP proteins become asymmetrically localized to opposite poles of the cell in response to Fz/PCP signaling, they are uniformly apically colocalized. Little is known about how the apical localization is maintained. We provide evidence that the PCP protein Diego (Dgo) promotes the maintenance of apical localization of Flamingo (Fmi), an atypical Cadherin-family member, which itself is required for the apical localization of the other PCP factors. This function of Dgo is redundant with Prickle (Pk) and Strabismus (Stbm), and only appreciable in double mutant tissue. We show that the initial membrane association of Dgo depends on Fz, and that Dgo physically interacts with Stbm and Pk through its Ankyrin repeats, providing evidence for a PCP multiprotein complex. These interactions suggest a positive feedback loop initiated by Fz that results in the apical maintenance of other PCP factors through Fmi.

Key words: *Drosophila*, Eye, PCP, *Vang*, *pk*, *Stbm*

Introduction

Epithelial cells are polarized apicobasolaterally and within the plane of the epithelium. The latter is known as planar cell polarization (PCP). PCP is evident in many tissues in vertebrates and invertebrates, and is often central to the development and function of an organ (Adler, 2002; Djiane et al., 2000; Keller, 2002; Mlodzik, 2002; Wallingford et al., 2002; Wallingford et al., 2000).

In *Drosophila*, PCP manifests itself in many adult tissues, most notably the eye, wing, notum (dorsal thorax) and abdomen (Adler, 2002; Casal et al., 2002; Mlodzik, 2002; Uemura and Shimada, 2003). Frizzled (Fz), which is the founding member of the seven-pass transmembrane Fz-receptor family of Wnt receptors (Bhanot et al., 1996; Vinson and Adler, 1987) requires Dishevelled (Dsh), a multi-domain cytoplasmic protein, to transduce signals (Boutros and Mlodzik, 1999). Downstream of Dsh, the Wnt/Fz signaling pathway bifurcates into two distinct pathways: the canonical Wnt/β-catenin pathway and the Fz/PCP pathway (reviewed by Mlodzik, 2002; Veeman et al., 2003). In addition, a conserved group of genes is involved in PCP generation by regulating Fz/PCP signaling. These genes include the atypical cadherin *flamingo* [*fmi*; also known as *stan* – FlyBase (Chae et al., 1999; Usui et al., 1999)], the cytoplasmic LIM-domain protein prickle [*pk* (Gubb et al., 1999)], the four-pass transmembrane protein Strabismus [*stbm*; also known as *Van Gogh* (*Vang* – FlyBase) (Chae et al., 1999; Taylor et al., 1998; Usui et al., 1999; Wolff and Rubin, 1998)] and Diego [see below (Feiguin et al., 2001)].

In the *Drosophila* wing, PCP signaling leads to the emergence of an actin hair at the distal vertex of each cell (with respect to the body). Although the PCP proteins are initially distributed uniformly around the apical cortex of each wing cell, as development and PCP establishment progress, these proteins are sorted towards either the distal (e.g. Fz, Dsh), the proximal (e.g. Stbm, Pk) or both (e.g. Fmi) cell margins (Axelrod, 2001; Bastock et al., 2003; Strutt, 2001; Tree et al., 2002; Usui et al., 1999). The actin hair emerges distally as a final outcome of the PCP protein distribution (Adler, 2002).

In the fly eye, PCP is reflected in the precise arrangement of ommatidia with respect to the anteroposterior (AP) and dorsoventral (DV) axes (Fig. 1A). The AP orientation follows the directed progression of a morphogenetic furrow (MF), leaving in its wake a series of ommatidial preclusters (Wolff and Ready, 1993). The precluster that emerges from the MF includes the precursors for the photoreceptors R2, R3, R4, R5 and R8. Initially, the R3/R4 cells are symmetrically positioned within the cluster (Fig. 1A). At this stage, Fz/PCP signaling breaks the initial symmetry within the R3/R4 pair and specifies their individual fates as two distinct photoreceptors (Adler, 2002; Mlodzik, 1999; Mlodzik, 2002). Following R3 and R4 cell fate determination, preclusters begin a 90° rotation in opposite directions in each half of the eye field (Fig. 1A,B). At the end of ommatidial rotation, the symmetric photoreceptor arrangement is broken and ommatidial chirality is established by the specific arrangement of the R3 and R4 photoreceptors (Fig. 1A).

During PCP establishment and R3/R4 cell fate specification,

it is thought that Fz/PCP signaling activity is graded: highest at the DV midline or the equator, and decreasing towards the poles. Although it remains unclear how a Fz/PCP activity gradient is generated, the transmembrane protein Four Jointed and the cadherins Fat and Dachsous have been implicated in this process (Ma et al., 2003; Yang et al., 2002; Zeidler et al., 1999; Rawls and Wolff, 2002). Within each precluster, Fz/PCP signaling is activated to higher levels in the R3 precursor, which is initially closer to the equator, when compared with the R4 precursor. This results in increased *Delta* (*Dl*) expression in R3, leading to activation of its ligand, Notch, in the neighboring R4 cell (Cooper and Bray, 1999; Fanto and Mlodzik, 1999; Tomlinson and Struhl, 1999; Zheng et al., 1995). Thus, the correct chirality decision and the direction of rotation are dependent on the correct R3/R4 cell fate decision.

The PCP gene *diego* (*dgo*) encodes a cytoplasmic protein with six Ankyrin repeats at its N-terminal region (Feiguin et al., 2001). The Ankyrin repeat motif has been implicated in membrane targeting of proteins (Bennett and Chen, 2001). Dgo has been shown to colocalize with and depend on Fmi for membrane recruitment. In addition, previous studies in the eye have shown that *dgo* mutants dominantly enhance a *fmi* GOF phenotype (Das et al., 2002; Feiguin et al., 2001). However, the role of Dgo in Fz/PCP signaling or its regulation has not yet been established.

We provide evidence that *dgo* is required to maintain the apical localization of other PCP factors. We demonstrate that Dgo is redundant to Pk and Stbm in this context, maintaining the apical localization of Fmi, following its Fz-dependent membrane recruitment. This role of Dgo, Pk and Stbm is supported by physical interactions between Pk and Stbm with Dgo. These data suggest a positive feedback loop initiated by Fz that results in the apical maintenance of all the other PCP factors (Fmi, Stbm, Pk, Dgo and Dsh).

Materials and methods

Fly strains and genetics

Overexpression studies were performed using the Gal4/UAS system (Brand and Perrimon, 1993), or by direct expression of the *dgo*-coding sequence in a modified *sev*-enhancer vector. Transgenic flies were generated by standard P-element mediated transformation (Spradling and Rubin, 1982). Interaction crosses were grown at 29°C and w^{1118} was used as control. For imaginal disc staining, the respective mutant chromosomes were established over the *TM6B* or *SM5a:TM6B* balancers. The flip-out clones of *UAS-GFP-Dgo* were generated using the *hsFLP, actin>CD2>Gal4* strains as described (Pignoni and Zipursky, 1997) and marked with UAS-*lacZ*.

Mutant alleles used were dgo^{308}, dgo^{380} (Feiguin et al., 2001), fmi^{E59}, fmi^{E45} (Lu et al., 1999), $pk\text{-}sple^{13}$, $stbm^{6cn}$, dsh^{1}, dsh^{v26}, fz^{R52} and fz^{K21} (http://flybase.bio.indiana.edu).

Immunohistochemistry and histology

Primary antibodies were: mouse anti-Fmi, rat anti-Dsh (generous gifts of T. Uemura; (Usui et al., 1999), rabbit anti-Dgo (Feiguin et al., 2001), rabbit anti-Stbm (Rawls and Wolff, 2003), rabbit anti-Pk (Tree et al., 2002), rabbit anti-Bar (gift from K. Saigo), rat anti-Sal (gift from R. Barrio) and anti-β-gal (Cappel, Promega). The β-Gal lines used were $Dl\text{-}lacZ^{1282}$ (from Marc Haenlin) and *svp-lacZ* (Baker et al., 1990). Rhodamine phalloidin (Molecular Probes) was used to visualize actin. Secondary antibodies coupled to fluorochromes were from Jackson Laboratories. Imaginal disc staining were performed as described (Fanto et al., 2000; Feiguin et al., 2001). Discs were mounted in Mowiol and viewed with a Leica confocal microscope; images were assembled in Adobe Photoshop. Confocal images shown are single optical sections.

Tangential eye sections were prepared as described (Tomlinson et al., 1987). For genetic interaction analysis, eyes were sectioned at the equatorial region and ommatidia scored for polarity. Three to 12 sections from independent eyes were scored for each genotype.

Molecular biology and biochemistry

To create pCRIITopo_Dgo and pCRIITopo_DgoAnk, Dgo cDNA was amplified with primers Dgo_upper_Not (TATGCGGCC-GCGATGCAGCATGGATCCTCC) and Dgo_AnkStop_Sal (ATAGTCGACTCATTTCTCCTTGCGATTCCG) or Dgo_lower_Sal (ATAGTCGACTCAAACTAGACTCGAGACATT), respectively, and cloned into pCRIITopo according to instructions of the manufacturer (Invitrogen). Inserts were then cloned as *Not*I(blunt)/*Sal*I fragments into the *Nsi*I(blunt)/*Xho*I sites of pβTH (Jenny et al., 2003) to give pβTH_Dgo and pβTH_DgoAnk. pGex4TI_DgoAnk was made by cloning the *Not*I(blunt)/*Sal*I fragment of pCRIITopo_DgoAnk into the *Bam*HI(blunt)/*Xho*I sites of pGex4TI. All other constructs are as described previously (Jenny et al., 2003). In vitro translations and GST pull-downs were carried out as described previously (Jenny et al., 2003). pEGFP-Dgo was made by cloning the *Not*I(blunt)/*Sal*I fragment of pCRIITopo_Dgo into the *Bgl*II(blunt)/*Sal*I sites of pEGFP_C1 (Clontech). GFP-Dgo was then transferred into *Spe*I/*Xba*I(blunt) sites of pUASP (Rorth, 1998) as *Nhe*I/*Sal*I(blunt) fragment. Sixty- to 80-hour-old larvae grown at 25°C, were heat-shocked for 1 hour at 38°C to induce Gal4 expressing flip-out clones. After the heat shock, larvae were kept at 18°C until dissection of the larval eye and pupal wing discs. Wing discs were stained as described (Feiguin et al., 2001).

To create pCRIITopo_Dgo and pCRIITopo_DgoAnk, Dgo cDNA was amplified with primers Dgo_upper_Not (TATGCGGCCGCGAT-GCAGCATGGATCCTCC) and Dgo_AnkStop_Sal (ATAGTCGA-CTCATTTCTCCTTGCGATTCCG) or Dgo_lower_Sal (ATAGTC-GACTCAAACTAGACTCGAGACATT), respectively, and cloned into pCRIITopo according to instructions of the manufacturer (Invitrogen). Inserts were then cloned as *Not*I(blunt)/*Sal*I fragments into the *Nsi*I(blunt)/*Xho*I sites of pβTH (Jenny et al., 2003) to give pβTH_Dgo and pβTH_DgoAnk. pGex4TI_DgoAnk was made by cloning the *Not*I(blunt)/*Sal*I fragment of pCRIITopo_DgoAnk into the *Bam*HI(blunt)/*Xho*I sites of pGex4TI. All other constructs are described elsewhere (Jenny et al., 2003). In vitro translations and GST pull-downs were carried out as described previously (Jenny et al., 2003).

Results

Diego is required for PCP establishment and has a characteristic PCP protein localization pattern in the eye

Loss-of-function mutant *dgo* eyes show typical PCP defects that include randomized chirality, and misrotated and symmetrical ommatidia. These defects are reminiscent of the phenotype of other primary PCP genes, except that in the dgo^{-} mutants, a higher percentage of ommatidia remain as symmetrical clusters (Fig. 1D, ~30% symmetrical clusters in dgo^{-} compared with 10% in fz^{-}). Similarly, overexpressed Dgo in the developing 3rd instar eye disc causes a typical gain-of-function PCP phenotype (not shown). Furthermore, the analysis of the orientation of preclusters in dgo^{-} clones in larval eye imaginal disc (with antibodies to Spalt, marking R3/R4 cells, and Bar, marking R1/R6 cells) revealed an abnormal orientation of the photoreceptor preclusters from early developmental stages (Fig. 1E; not shown). Taken together,

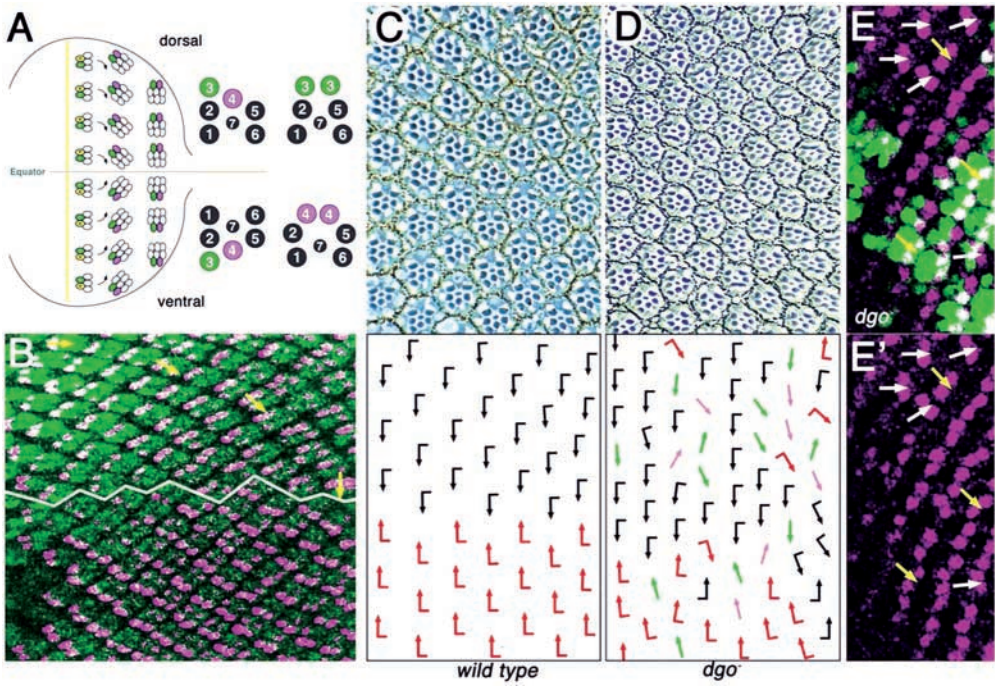

Fig. 1. The *dgo* eye phenotype. (A) Schematic drawing of 3rd instar larval eye imaginal disc, with the morphogenetic furrow (MF; yellow) and the DV midline (the equator; gray) indicated. Anterior is leftwards and dorsal upwards in this and all subsequent figures. Initially, ommatidial preclusters are symmetrical and organized in the AP axis. Subsequently, they rotate 90° with respect to the equator; at the end of this process chirality is established by the positions of R3 and R4. (Right) Schematic presentation of chiral organization of dorsal and ventral adult ommatidia; in addition to the chiral forms, symmetrical clusters with R3/R3 or R4/R4 cell pairs as found in PCP mutants are shown. R3 cells are highlighted in green and R4s in magenta. (B) Partial view of a developing eye imaginal disc demonstrating the regularity of polarity establishment. Ommatidial clusters are marked with anti-Elav (green; labeling all photoreceptors) and *svp-lacZ* [magenta: *svp* is expressed initially in R3/R4 (see left side of panel) and later also in R1/R6 at weaker levels]. The MF is on left side adjacent to field shown. Orientation of some dorsal ommatidial preclusters is highlighted with yellow arrows; white line marks the equator. (C,D) Tangential sections of adult eyes with the respective schematic presentations of the genotypes indicated. Wild-type dorsal and ventral ommatidial arrangement is represented by black and red arrows, respectively; symmetrical R3/R3 and R4/R4 ommatidia are represented by green and magenta arrows, respectively. (C) Wild-type eye with regular arrangement of dorsal and ventral ommatidia around equator. (D) dgo^{380} eye (null allele). The equatorial arrangement is disturbed with a random arrangement of both chiralities (black and red arrows), and the presence of many symmetrical clusters of both R3/R3 and R4/R4 types (green and magenta arrows). (E,E′) Confocal microscopy images of mosaic 3rd instar eye disc, with dgo^- tissue marked by absence of green (GFP); anti-Bar labeling R1/R6 (magenta) highlights orientation of clusters. (E′) Single channel showing Bar staining. Orientation defects of the preclusters are visible from early stages in mutant tissue. Examples with abnormal orientation are indicated with white arrows; yellow arrows indicate wild-type orientation for comparison.

these data and the wing analysis (Feguin et al., 2001) indicate that *dgo* behaves like a primary PCP gene, revealing a characteristic role in PCP establishment.

To better define the role of Dgo in PCP establishment, we next analyzed Dgo localization in 3rd instar eye discs. Dgo is detected apically at the membrane in all cells ahead of and behind the MF (Fig. 2A; not shown). The initial uniform apical localization changes posterior to the MF in rows 2 to 3 in the 5 cell precluster (Fig. 2A). At this stage, Dgo is detected at higher levels in R3/R4 cells within the dorsoventral axis and, in particular, at the membranes between R3 and R4. Dgo is absent from membranes where the R3/R4 cells abut the R2/R5 pair. By row 5, Dgo is maintained at the border between the R3/R4 cells, whereas it is now detected at lower levels in other membrane regions of R3 and becomes enriched to higher levels in R4 (Fig. 2A). The asymmetric enrichment in the R4 cell becomes resolved by row 6 and persists through row 10. In addition, Dgo is detected at high levels at the posterior side of the R2/R5 and R8 cells from row 2 onwards (Fig. 2A). In summary, these data indicate that the localization of Dgo has a pattern characteristic of other PCP proteins in the eye disc.

Diego is localized to the R3 side of the R3/R4 cell boundary

The PCP genes so far analyzed in detail show an asymmetric localization across the R3/R4 membranes as the result of PCP signaling. Thus, for example, although initially on both sides of the R3/R4 membrane, Fz becomes subsequently enriched to the R3 side. By contrast, Stbm becomes enriched on the R4 side (Strutt et al., 2002). This asymmetric localization is also evident in the relevant stages of PCP establishment in the wing, where Fz and Stbm are localized to the opposing sides of the proximal/distal cellular boundary (Strutt et al., 2002). To determine the precise localization of Dgo in this context, we have generated transgenic flies with a functionally active GFP-Dgo (it rescues the dgo^- phenotype, not shown), and analyzed its localization in mosaic clusters (see Materials and methods for details). This analysis revealed that GFP-Dgo is first detected on both sides of the R3/R4 membrane (Fig. 2B,C), but subsequently becomes restricted to the R3 side of the R3/R4 cell membrane (Fig. 2D,E; in addition, it is detected in R4 on the polar side, like other PCP genes). Consistent with this observation, *dgo* shows a genetic requirement in R3 for correct chirality establishment (J.R.K. and M.M., unpublished). Similarly, in pupal wings when the localization of the PCP factors is resolved within the proximodistal axis, GFP-Dgo is enriched on the distal side of the proximal cell, and is largely absent from the opposing membrane (Fig. 2F,F′). A schematic presentation of these localization studies is shown in Fig. 2G-I.

Taken together, these data indicate that Dgo always localizes

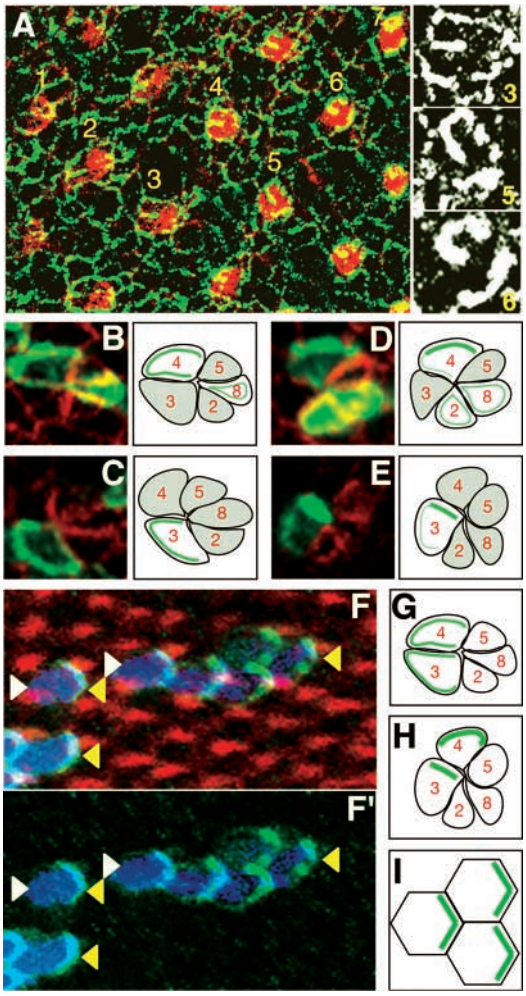

Fig. 2. Localization of Dgo during PCP establishment in the eye. Anterior is leftwards and dorsal upwards in all panels except F and I, where proximal is leftwards. (A) Single apical confocal microscopy section showing ommatidial rows 1-7 stained with anti-Dgo (green) and phalloidin (highlighting F-actin, red) to mark the center of each cluster. Morphogenetic furrow (anterior) is on the left of the panel and the equator is at the bottom. (Right panels) Monochrome higher magnifications of single clusters from row 3, row 5 and row 6 (as indicated). Dgo is first detected apical at the membrane in all cells ahead of and posterior to MF (up to row 2). More posteriorly, the initial uniform apical localization changes (row 3) within five cell preclusters, and Dgo is present at higher levels in R3/4 cells within the equatorial-polar (DV) axis. (Row 5) Dgo is maintained at the border between the R3/R4 cells, but it is now detected less in parts of R3 and at higher levels in R4. (Row 6) The R4 specific enrichment is now complete and persists through row 10. Whereas there is no Dgo detected at membranes where R3/R4 abut the R2/R5 pair, Dgo is enriched at the opposing R8, R2/R5 membranes. (B-D) Mosaic analysis of GFP-Dgo to determine the precise localization of Dgo at the R3/R4 cell boundary. GFP-Dgo is in green, anti-DE Cadherin is in red. Right side panels show a schematic of actual clusters on the left. Cells are numbered according to their position; cells shown in white express GFP-Dgo in the given cluster; GFP-Dgo at localization membranes is highlighted with green lines. (B,C) Mosaic clusters in row 3 with either R4 (B) or R3 (C) expressing GFP-Dgo. Dgo localization reflects a horseshoe-like pattern in both R3 and R4 cells. (D,E) Mosaic clusters in rows 5-6, with (again) either R4 (D) or R3 (E) expressing GFP-Dgo. Dgo is now enriched only at the R3 side of the R3/R4 cell boundary and the polar side of R4 (very similar to the localization of Fz). (F) GFP-Dgo (green) clones in pupal wings at 60-80 hours at 18°C. *lacZ* (blue) marks the cells that express GFP-Dgo; F-actin (phalloidin, red) labels the growing actin hairs; proximal is leftwards. GFP-Dgo localizes to the distal membrane of each cell that expresses it. (G-I) Schematic summary presentation of the Dgo localization patterns in developing eye (G, row 3; H, row 6) and pupal wing (I) cells; again, Dgo shows the same localization pattern as Fz and Dsh.

in a manner similar to Fz and Dsh both in the eye, on the R3 side of the R3/R4 cell boundary, and in the wing on the distal side of the pupal wing cell.

Dgo localization is promoted by Fz

A mutation in a PCP gene can affect the localization of other PCP proteins in three distinct ways in the eye: (1) asymmetric R4-like enrichment occurs but is random with respect to the R3/R4 precursor cell (reflecting chirality flips); (2) no asymmetric pattern is observed, but apical localization is maintained; and (3) apical localization is compromised.

As Dgo is predicted to be a cytoplasmic protein, a question of particular interest is how it becomes recruited to the membrane. Previous studies in the wing and eye have shown that Dgo localization is affected by *fmi*, but Fmi itself was not sufficient to recruit Dgo to the membrane (Das et al., 2002; Feiguin et al., 2001).

In *fz*-null clones, Dgo completely loses its apical membrane localization (Fig. 3A,B) and, strikingly, this is evident not only posterior to the MF (Fig. 3B), but also anterior to the MF prior to a PCP requirement (Fig. 3A). This *fz* requirement is unique to Dgo, as *fz* has no effect or a different effect on the localization of Pk, Fmi and Stbm: the apical localization of Pk is not perturbed significantly, except for the loss of the characteristic PCP protein localization pattern, as seen in the case of Fmi in *fz* mutants (Fig. 3E; not shown) (Das et al., 2002). In addition, Dgo seems to be found at higher levels at the clone borders (vertical arrowheads in Fig. 3B), suggesting that a difference in Fz signaling levels promotes PCP complex formation, and this is also observed for Fmi localization (Das et al., 2002). Dgo is much less affected in mutant clones for any other PCP gene: in *fmi*$^{-}$ clones, residual Dgo is still present at the membrane, although it largely loses its membrane association (Das et al., 2002; Feiguin et al., 2001); in *pk*$^{-}$ and *stbm*$^{-}$ tissue, Dgo localization is only slightly affected (Fig. 3G,H) with a short delay (approximately one row) in the asymmetric R4-like enrichment. In tissue that is *dgo*$^{-}$, none of the other PCP factors is affected and they localize normally to the apical cortex, resulting in the typical asymmetric, albeit randomized, R4-like enrichment (Fig. 3C,D,F) (Das et al., 2002).

In summary, these data suggest that while Fz is the key PCP protein that recruits Dgo to the apical membrane cortex, Fz localization is unaffected in *dgo*$^{-}$ tissue, indicating that *dgo* acts downstream of *fz* for its localization. In addition, Dgo alone does not affect the apical or asymmetric localization of other PCP proteins (see below).

Dgo, Pk and Stbm promote the apical localization of Fmi and Fz

Previous studies have suggested that Fz and Fmi promote each other's asymmetric distribution, but that Fmi remains apically

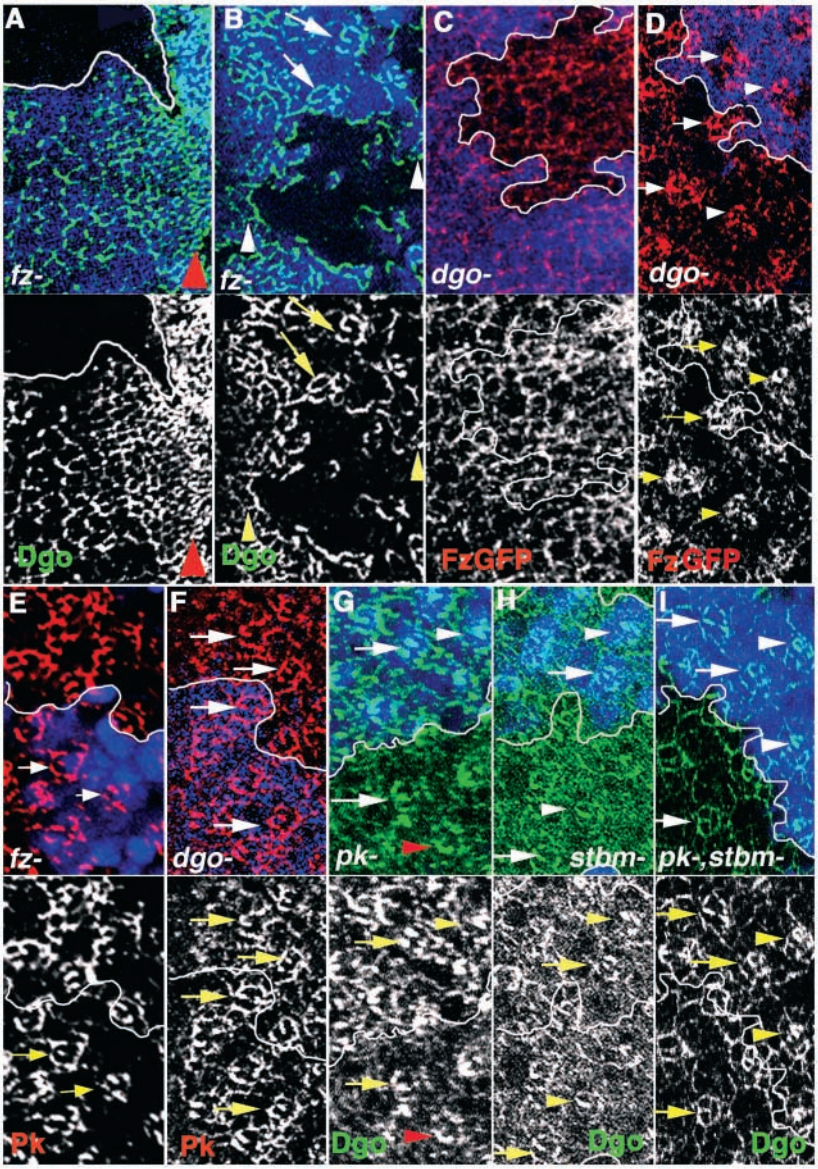

Fig. 3. Dgo membrane association requires *fz*. Panels show single confocal sections; anterior is leftwards and the equator is at the bottom (MF is at the left edge of each panel, except in A where it is on the right, marked by the red arrowhead). Mutant tissue is marked by absence of β-gal staining or GFP (blue). White/yellow arrows indicate examples of clusters with PCP protein localization in R3/R4 cell pair (equivalent to row 3 or 4, see also Fig. 2A) and arrowheads in C-E indicate the asymmetric R4-like enrichment (around row 5-6). Green channel: anti-Dgo (in A-E). Red channel: Fz-GFP in C and D; Pk in panels E and F. Clones of null alleles of the respective genes are shown. (A) fz^- clone anterior to MF, which is marked with red arrowhead. Strikingly, also anterior to the MF, Dgo is delocalized in fz^{R52} tissue [Dgo is apically localized in all wd-type cells (blue), ahead of the MF]. (B) fz^- tissue posterior to MF; apical membrane-associated Dgo localization is absent in fz^- cells (examples in wild-type area are indicated by white arrows). Dgo is enriched at membranes between fz^+ and fz^- cells (e.g. vertical arrowhead). (C) dgo^- clone anterior to MF. There is no change in apical Fz-GFP localization in mutant tissue [compare with wild-type cells (blue)]. (D) dgo^- tissue posterior to MF. Apical membrane-associated Fz-GFP localization is not affected in dgo^- cells (examples of preclusters in wild-type and mutant areas are indicated by white arrows). (E) Pk localization in fz^- tissue posterior to MF. While apical levels of Pk localization are unaffected, the characteristic asymmetric PCP localization pattern is not observed. (F) Pk localization in dgo^-: apical localization pattern of Pk in mutant tissue is unchanged. (G,H) Dgo localization in pk^- and $stbm^-$ clones: the Dgo pattern is as in wild type. Although Dgo displays the R4 asymmetry as in wild type, the R4-like enrichment to either equatorial or polar side is randomized [e.g. in the equatorial cell (red arrowhead), reflecting chirality flips], mimicking the adult phenotype of random chirality. (I) pk^-, $stbm^-$ tissue: apical Dgo localization is reduced and characteristic R4-like pattern is not resolved.

localized in fz^- tissue (Das et al., 2002; Strutt, 2001). Fmi has also been shown to promote the apical and asymmetric localization of the cytoplasmic PCP proteins Dgo, Dsh and Pk (Das et al., 2002; Strutt et al., 2002). In addition, in the eye *fz* again affects the asymmetric localization of Stbm, Fmi and Pk, but not their apical localization (not shown) (Das et al., 2002; Strutt et al., 2002). Nevertheless, very little is known about how the apical localization of Fmi and Fz themselves is established and, importantly, maintained prior to PCP signaling in the eye or the wing.

In order to address this issue, we have analyzed the localization of Fz and Fmi in all single and in several double mutant PCP gene combinations. Single mutant *pk* and *stbm* clones show no significant defects in apical or asymmetric Fz or Fmi localization (Fig. 4A; not shown) (Bastock et al., 2003; Das et al., 2002; Strutt et al., 2002), indicating that *stbm* and *pk* alone are not crucial for apical Fmi or Fz localization. However, in dgo^-, pk^- double mutant clones (in 3rd instar eye discs anterior and posterior to the MF) the apical localization of Fmi and Fz is strongly reduced (Fig. 4B,C; not shown). A similar effect is observed in dgo^-, $stbm^-$ double mutant clones (Fig. 4D,E; not shown), suggesting that Dgo acts in a redundant manner with Pk and Stbm for this function. In contrast to dgo^-, pk^- and dgo^-, $stbm^-$ double mutants, pk^-, $stbm^-$ double mutant tissue shows a different effect. Whereas the apical localization of Fmi and Fz anterior to the MF is reduced (Fig. 4F; not shown), similar to, for example, dgo^-, pk^- double mutant clones, apical Fmi and Fz localization is basically unaffected posterior to the MF (Fig. 4F,G). Although, the apical localization of Fmi was lost, Fmi protein was present in all single and double mutant backgrounds at comparable levels to wild type (determined by western blot analysis; not shown).

These data suggest that there is a degree of redundancy among the PCP genes and that certain requirements for their localization can be mediated by more than one core PCP gene. In contrast to the single mutants of either *stbm*, *pk* or *dgo*, or double mutants of $stbm^-$, pk^- (posterior to the MF), where localization of Fmi or Fz is not significantly affected, the dgo^-,

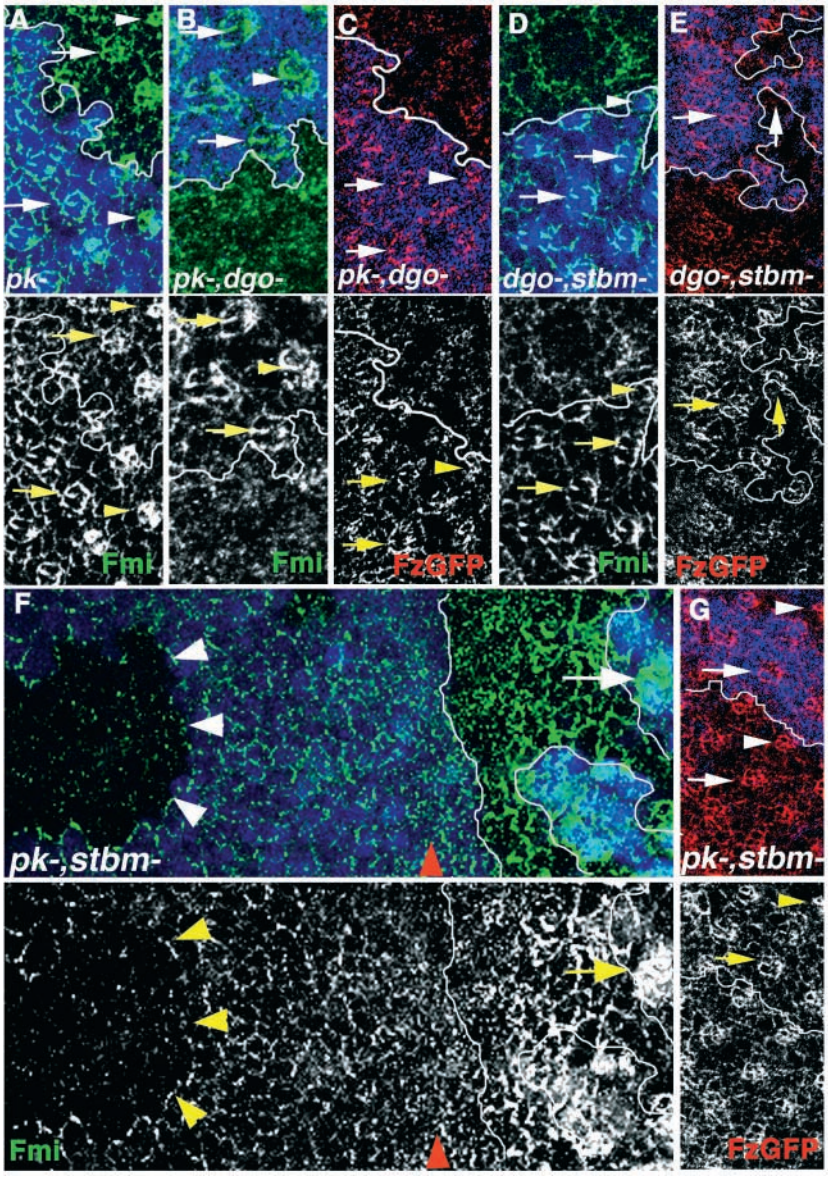

Fig. 4. Dgo, with Pk and Stbm, promotes the apical localization of Fmi and Fz. Apical confocal sections are shown; anterior is leftwards and the equator at bottom. MF is at left margin of panels, except in F where it is indicated by red arrowhead. Mutant tissue is marked by absence of β-gal staining or GFP (blue). White/yellow arrows indicate PCP protein localization in R3/R4 pair (~row 3 or 4) and arrowheads indicate the R4-like enrichment (row 5 and posterior), except in F where it indicates clones ahead of MF. Fmi (green) and Fz-GFP (red) localization is analyzed in mutant tissue of null alleles of the respective PCP genes. (A) *pk*⁻: no significant abnormalities in the apical localization of Fmi. (B) *pk*⁻, *dgo*⁻: loss of apical Fmi localization. (C) *pk*⁻, *dgo*⁻: reduction in apical Fz localization. (D) *dgo*⁻, *stbm*⁻: loss of apical Fmi localization (compare with A and B). (E) *dgo*⁻, *stbm*⁻: loss of apical Fz-GFP localization. The vertical arrow indicates a mosaic in which the R3 specific Fz-GFP staining is missing. (F) *pk*⁻, *stbm*⁻ mutant clones behind and ahead of MF (marked by red arrowhead): apical Fmi localization is lost in mutant tissue ahead of MF, similar to *pk*⁻, *dgo*⁻ and *pk*⁻, *stbm*⁻ double mutants (compare with B and C), but apical localization of Fmi is observed posterior to MF, although no clear pattern is detected. In *pk*⁻, *stbm*⁻ double mutant tissue there is a different effect on Fmi anterior and posterior to MF. (F) *pk*⁻, *stbm*⁻: apical Fz-GFP localization behaves like Fmi: it is unaffected posterior to MF (but lost anterior to MF, not shown).

stbm⁻ and *dgo*⁻, *pk*⁻ double mutant backgrounds always compromise apical Fmi and Fz localization throughout the eye disc. It is likely that these effects are mediated through a feedback loop via Fmi (see below and Discussion).

Dgo and Pk promote apical localization of Dsh and Stbm

To explore this observation of potential redundancy further, we analyzed Stbm and Dsh localization in *dgo*⁻, *pk*⁻ double mutant tissue. The localization of Dsh and Stbm is not significantly affected in *dgo*⁻ mutant clones (Fig. 5A,C). In *pk*⁻ mutants, Dsh and Stbm are localized apically, although this localization appears to be slightly diffused (Fig. 5D; not shown). Similarly, apical Dsh localization is not affected in *stbm*⁻ tissue in the eye [not shown; this is different from the wing (Bastock et al., 2003; Strutt et al., 2002)]. By contrast, neither Dsh nor Stbm are detected at apical membranes in *dgo*⁻, *pk*⁻ double mutant clones (Fig. 5B,E). As localization of Fmi (which also affects Stbm and Dsh localization; Fig. 5F) is similarly affected in the *dgo*⁻, *pk*⁻ double mutant background, this effect could be indirectly mediated via Fmi (see above) (Das et al., 2002; Strutt et al., 2002). The requirement of Fmi for the maintenance is further supported by the fact that in *fmi*⁻, the apical localization of Fz is significantly compromised both posterior and anterior to the furrow (Fig. 5G).

In summary, these observations raise an important question about the basis of the differences observed between the double and single mutant clones. A possible explanation for the differences in localization patterns could be that an initial complex is comprised of a number of factors, and the absence of one factor can be tolerated for some aspects of function, e.g. the maintenance of apical localization of Fmi and thus by inference also of the other PCP genes (see Discussion).

Dgo physically interacts with Pk and Stbm

To provide biochemical evidence for a PCP multiprotein complex, we tested for physical interactions between these factors in a yeast two-hybrid matrix with available PCP proteins (A.J. and M.M., unpublished). This initial test suggested that Dgo interacts physically with Pk and Stbm (data not shown). GST pull-down assays were used to confirm these interactions independently and map the interacting domains (Fig. 6). Using in vitro translated constructs of full-length Dgo and the Ankyrin repeat region of Dgo (Fig. 6A), we showed that Dgo-Ank is sufficient to interact with a stretch of 131 amino acids close to, but not including, the very C terminus of

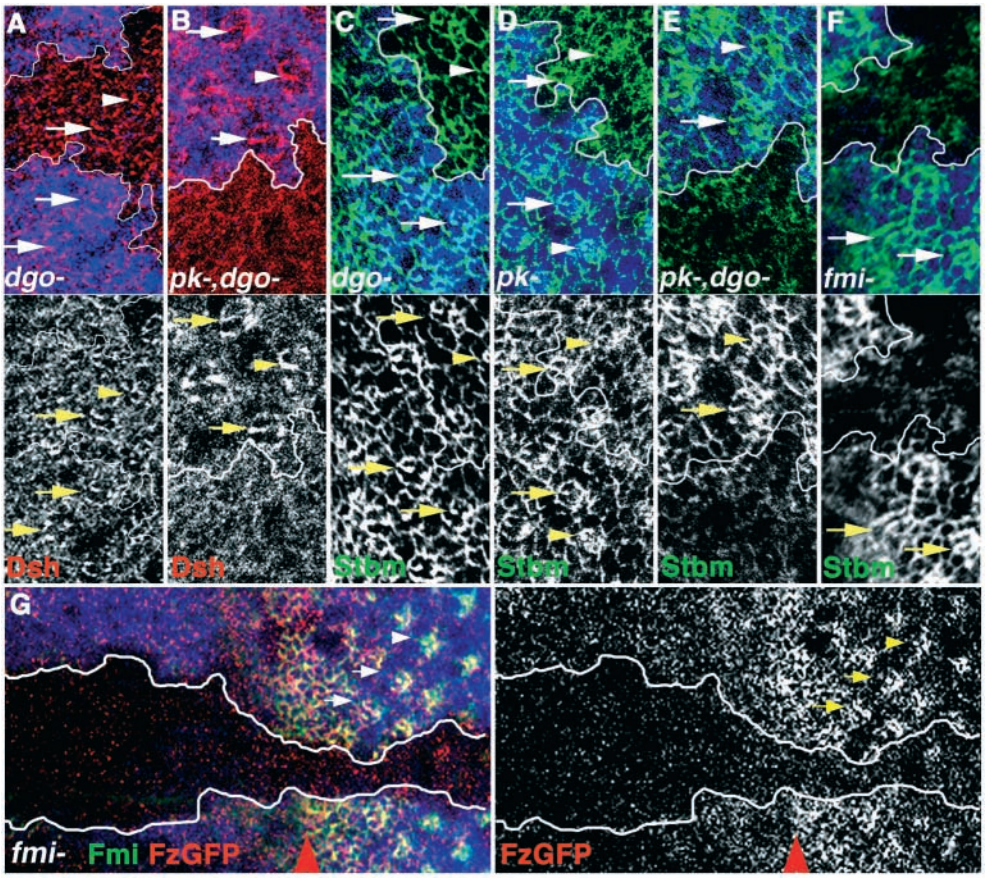

Fig. 5. Dsh, and Stbm localization in PCP mutants. Apical confocal sections with MF (anterior) at left edge and equator at bottom. MF is at the left margin of all panels, except in G, where it is indicated by red arrowheads. Mutant tissue is marked by absence of β-gal staining or GFP (blue). White/yellow arrows indicate PCP protein localization in R3/R4 pairs (rows 3 or 4) and arrowheads mark clusters with R4-like enrichment (row 5 onwards). Localization of Dsh and Fz-GFP (red) and Strabismus (green) are shown. Clones of null alleles of the respective PCP genes (as indicated) are shown. (A) *dgo*$^{-}$: no differences in Dsh localization are detected between wild-type and mutant tissue. (B) *pk*$^{-}$, *dgo*$^{-}$: loss of apical localization of Dsh. (C) *dgo*$^{-}$: no difference in Stbm localization between wild-type and mutant tissue. (D) *pk*$^{-}$: apical localization of Stbm is observed (although it is slightly reduced). (E) *pk*$^{-}$, *dgo*$^{-}$: loss of apical Stbm localization. (F) *fmi*$^{-}$: loss in apical localization of Stbm. (G) *fmi*$^{-}$: loss of apical Fz-GFP localization is observed.

Pk (Fig. 6A). Similarly, Dgo-Ank interacts with a Stbm domain of ~80 amino acids in its cytoplasmic tail (Fig. 6B). Interestingly, the regions of Pk and Stbm required for the interaction with Dgo-Ank are the same regions that mediate an interaction between Pk and Stbm themselves (Jenny et al., 2003).

The physiological relevance of the physical interactions between Dgo-Pk and Dgo-Stbm is further supported by genetic interaction data (for example, a GOF *stbm* phenotype is enhanced by *dgo* gene dose) (Jenny et al., 2003), and in vivo localization studies. Whereas in single mutant *pk*$^{-}$ or *stbm*$^{-}$ tissue Dgo localization was not affected (Fig. 3G,H), in *pk*$^{-}$, *stbm*$^{-}$ double mutant tissue Dgo was reduced at the apical cortex (Fig. 3I). Taken together, these data suggest it is likely that an initial multiprotein complex is required to maintain all PCP proteins apically and that redundancy exists between Dgo, Pk, and Stbm for this particular role (see Discussion).

Discussion

We demonstrate here that Dgo maintains a potential PCP complex through the apical localization of Fmi, which in turn is required for the apical localization of the other PCP factors, including Dgo. Interestingly, this function of Dgo is redundant with Pk and Stbm, and is only apparent in double mutant clones of Dgo in combination with either gene. This observation is supported by the molecular interaction between Dgo and Pk or Stbm.

Diego and the formation of a multiprotein PCP signaling complex

A crucial region for PCP signaling in the eye is in rows 2-5 in the 3rd instar larval disc behind the morphogenetic furrow (MF; see also Introduction). Four lines of evidence support this assumption: (1) cells that take part in PCP signaling (R3/R4) are specified as photoreceptor subtypes in this region (Wolff and Ready, 1991); (2) Frizzled-Notch signaling-dependent transcription in the R4 cell is initiated in this region, as detected by the *mδ0.5* reporter for the *E(spl)mδ* gene (Cooper and Bray, 1999); (3) the *sev*-enhancer, which is active in R3/R4 cells in this region, can drive a PCP gene in order to fully rescue the respective mutant phenotype (Boutros et al., 1998; Tomlinson and Struhl, 1999); and (4) in the region ahead of the MF to the first row behind it, the PCP proteins are uniformly apically localized in all cells, before they begin at row 2 to display the characteristic PCP protein localization pattern (e.g. Fig. 2A) (Das et al., 2002; Rawls and Wolff, 2003; Strutt et al., 2002).

Following their initial symmetric apical localization, the PCP factors become asymmetrically enriched across the respective cell boundaries in the proximodistal axis in the wing or the dorsoventral axis in the eye. Although several models have been proposed as to how these complexes might be formed and maintained, the mechanism behind the early aspect of PCP establishment remains largely unclear (Strutt, 2003; Tree et al., 2002). Our data suggest a complex mechanism that involves redundancy among several PCP genes (see model, Fig. 7).

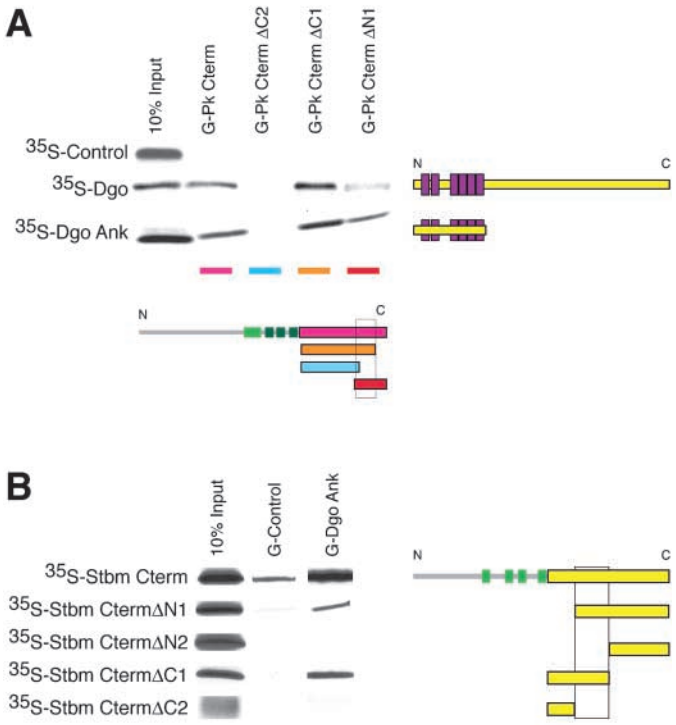

Fig. 6. Dgo physically interacts with Pk and Stbm in vitro. (A) Dgo Ankyrin repeats bind to a 131 amino acid fragment of Pk (white box in scheme). GST fusion proteins with fragments of the C terminus of Pk indicated at the top (color coded below, compare with scheme) were tested for binding to full-length Dgo (^{35}S-Dgo in vitro translated; marked yellow in the scheme on the right) or to its Ankyrin repeat region (^{35}S-Dgo Ank). An unrelated control (^{35}S-Control) does not bind to Pk. As a standard, 10% of the in vitro translated protein used for the binding reaction was loaded directly (10% input). The Pk region interacting with Dgo comprises residues 820-908. Purple boxes in Dgo scheme on right indicate the Ankyrin repeats and light and dark green boxes in scheme underneath indicate the PET and the three LIM domains of Pk, respectively. (B) Dgo Ankyrin repeats interact with Stbm. In vitro translated fragments of the C-terminal cytoplasmic region of Stbm (indicated on left and marked in yellow in scheme on right) were tested for their binding to a GST fusion protein of the Ankyrin repeats of Dgo (G-Dgo Ank) or to an unrelated fusion protein (G-Control). ^{35}S-Stbm CtermΔN2 and ^{35}S-Stbm CtermΔC2 define a region of 85 amino acids required for binding of Stbm to Dgo. Standard is as in A. Light green boxes in scheme on right indicate position of the predicted four transmembrane domains of Stbm.

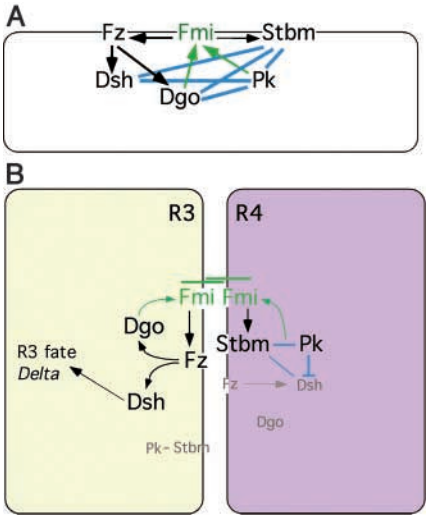

Fig. 7. (A) Model for maintenance of the apical PCP protein complex (prior to PCP signaling, e.g. anterior to MF). Known physical interactions are highlighted in blue (this work) (Tree et al., 2002; Jenny et al., 2003). The predicted Fmi-mediated complex, containing also Fz, Stbm and Dsh, is stable when either Dgo or Pk are removed, but unstable in the double mutant. (B) Proposed model for PCP signaling circuitry during PCP signaling, e.g. in R3/R4 cells. Fmi is maintained through Dgo function in R3 and Stbm/Pk in R4. Known physical interactions are in blue (Jenny et al., 2003; Tree et al., 2002). Factors depicted in gray are downregulated through PCP signaling at this stage. See text for details.

Based on the analysis of single mutant clones in the eye, only Fz and Fmi affect PCP gene localization in a general non-redundant manner (and Stbm affects Pk localization). The single and double mutant clone data indicate the following.

(1) Fz is required for membrane localization of Dgo (Fig. 2A,B) and this step precedes any apparent PCP signaling requirement. Fz also affects the apical localization of Dsh but not of Fmi, Pk, and Stbm significantly.

(2) Dgo alone does not affect the apical localization of other PCP genes, but instead it shares this function redundantly with Stbm and Pk.

(3) Pk alone does not affect the apical localization of other PCP proteins significantly, but does so in conjunction with Dgo and Stbm.

(4) Fmi is responsible for the apical localization of Fz (Strutt et al., 2002) (Fig. 5G).

In addition to these initial requirements for apical localization and maintenance, the subsequent asymmetric resolution of the respective PCP proteins to the R4 cell is affected and often delayed in mutant backgrounds (this work) (Strutt et al., 2002; Tree et al., 2002).

How is the initial apical localization of all these factors maintained? As outlined above, none of the single mutant PCP genes, except *fz* and *fmi*, has a significant effect on the whole complex. However, in double mutant clones for either *dgo* and *pk*, or *dgo* and *stbm*, localization of the PCP proteins is severely affected. Most strikingly, the apical localization of Fmi and Fz is affected in these double mutant combinations (Fig. 4B-E). In addition, the localization of Stbm and Dsh are also affected (Fig. 5B,E). This could be either a direct effect of Dgo and Pk or could be mediated through their effect on Fmi [as in *fmi*$^{-}$ tissue, Stbm and Dsh as well as Fz are reduced apically; Fig. 5F,G (Das et al., 2002)]. These data suggest that the cytoplasmic PCP proteins, which are initially recruited to the membrane by Fz (i.e. Dgo and Dsh) and Stbm (i.e. Pk), form a protein complex that is required to maintain Fmi apically (Fig. 7A). This interpretation is supported by our observation that Dgo physically interacts with Stbm and Pk, and thus possibly stabilizes the initial complex (Fig. 6). Thus, our studies reveal that Dgo, Stbm and Pk are required to maintain apical Fmi localization, possibly through the physical interactions among themselves and possibly other PCP factors, during the early stages preceding PCP signaling (i.e. anterior to MF in eye). In turn, apical Fmi promotes the maintenance

of an initial PCP complex at adjacent cell membranes to facilitate their signaling specific interactions.

We can speculate on further implications of these data. During later stages of PCP signaling, the localization of the PCP factors is resolved into two types of complexes on adjacent cell membranes. The differential localization of either Fz/Dgo or the Stbm/Pk complex in the neighboring cells (R3 versus R4) suggests that asymmetric localization of PCP factors is maintained across the border of the R3 and R4 cells in the eye and across proximodistal cell borders in the wing (Tree et al., 2002). In the eye, the PCP proteins analyzed in this manner indeed localize to specific sides of the R3/R4 cell border (Fig. 2) (Strutt et al., 2002). Similarly, proximodistal localization in the wing correlates with the respective R3/R4-specific localization. For example, the localization of Fz and Diego in the distal side of a wing cell correlates with the localization on the R3 side of the R3/R4 border; conversely, Stbm localization to the proximal side of a wing cell correlates with its localization on the R4 side of the R3/R4 border (Jenny et al., 2003; Tree et al., 2002). The localization to either the R3 or R4 side also corresponds to the genetic requirements in either cell, as established in mosaic analyses (Fanto and Mlodzik, 1999; Tomlinson and Struhl, 1999; Wolff and Rubin, 1998; Zheng et al., 1995). Thus, as Dgo, which is initially recruited by Fz, localizes to R3 and the pk/stbm complex localizes to R4, it is likely that at later stages during PCP signaling (posterior to MF) Fmi localization is maintained and stabilized through feedback loops on both sides of the R3/R4 boundary (see model in Fig. 7B).

A prediction from such a scenario is that Fz/Dgo are performing this function in R3 and the Stbm/Pk complex (Jenny et al., 2003) in R4. As Fmi is known to function as a homophilic cell-adhesion molecule (Usui et al., 1999), the removal of the feedback loop on one side could be overcome through the homophilic recruitment of Fmi from the other side. Only when both feedback loops are weakened on either side, can Fmi localization become affected (Fig. 7B). This is supported by the different effects of the respective double mutants posterior to the MF; those that affect both sides of the R3/R4 boundary, e.g. *dgo* and *stbm* (R3side/R4side) or *dgo* and *pk* (R3side/R4side) can cause Fmi delocalization, whereas double mutants affecting only one cell, e.g. *pk* and *stbm* (both R4side), have no significant effect.

We are grateful to T. Uemura, T. Wolff and J. Axelrod for generously providing us with Fmi, Stbm and Pk reagents. We thank J. Treisman, P. Adler, D. Strutt, R. Barrio, K, Basler, S. Bray, B. Dickson, E. Knust, T. Laverty, G. Rubin, K. Saigo, the Developmental Studies Hybridoma Bank and the Bloomington Stock Center for fly strains and antibodies. Microscopy was performed at the MSSM-Microscopy Shared Resource Facility, supported by a NIH-NCI shared resources grant (1 R24 CA095823-01); we thank P. Carmen and S. Henderson for their assistance at the MSSM the microscopy facility. We thank all members of the Mlodzik laboratory, and F. Cole for helpful discussions and comments on the manuscript. This research was supported by the NIH/NIGMS (grant RO1 GM62917 to M.M.).

References

Adler, P. N. (2002). Planar signaling and morphogenesis in Drosophila. *Dev. Cell* **2**, 525-535.

Axelrod, J. D. (2001). Unipolar membrane association of Dishevelled mediates Frizzled planar cell polarity signaling. *Genes Dev.* **15**, 1182-1187.

Baker, N. E., Mlodzik, M. and Rubin, G. M. (1990). Spacing differentiation in the developing Drosophila eye: a fibrinogen-related lateral inhibitor encoded by *scabrous*. *Science* **250**, 1370-1377.

Bastock, R., Strutt, H. and Strutt, D. (2003). Strabismus is asymmetrically localised and binds to Prickle and Dishevelled during Drosophila planar polarity patterning. *Development* **130**, 3007-3014.

Bennett, V. and Chen, L. (2001). Ankyrins and cellular targeting of diverse membrane proteins to physiological sites. *Curr. Opin. Cell Biol.* **13**, 61-67.

Bhanot, P., Brink, M., Samos, C. H., Hsieh, J.-C., Wang, Y., Macke, J. P., Andrew, D., Nathans, J. and Nusse, R. (1996). A new member of the *frizzled* family from *Drosophila* functions as a Wingless receptor. *Nature* **382**, 225-230.

Boutros, M. and Mlodzik, M. (1999). Dishevelled: at the crossroads of divergent intracellular signaling pathways. *Mech. Dev.* **83**, 27-37.

Boutros, M., Paricio, N., Strutt, D. I. and Mlodzik, M. (1998). Dishevelled activates JNK and discriminates between JNK pathways in planar polarity and *wingless* signaling. *Cell* **94**, 109-118.

Brand, A. H. and Perrimon, N. (1993). Targeted gene expression as a means of altering cell fates and generating dominant phenotypes. *Development* **118**, 401-415.

Casal, J., Struhl, G. and Lawrence, P. A. (2002). Developmental compartments and planar polarity in Drosophila. *Curr. Biol.* **12**, 1189-1198.

Chae, J., Kim, M. J., Goo, J. H., Collier, S., Gubb, D., Charlton, J., Adler, P. N. and Park, W. J. (1999). The Drosophila tissue polarity gene starry night encodes a member of the protocadherin family. *Development* **126**, 5421-5429.

Cooper, M. T. D. and Bray, S. J. (1999). Frizzled regulation of Notch signalling polarizes cell fate in the *Drosophila* eye. *Nature* **397**, 526-529.

Das, G., Reynolds-Kenneally, J. and Mlodzik, M. (2002). The atypical cadherin Flamingo links Frizzled and Notch signaling in planar polarity establishment in the Drosophila eye. *Dev. Cell* **2**, 656-666.

Djiane, A., Riou, J., Umbhauer, M., Boucaut, J. and Shi, D. (2000). Role of frizzled 7 in the regulation of convergent extension movements during gastrulation in Xenopus laevis. *Development* **127**, 3091-3100.

Fanto, M. and Mlodzik, M. (1999). Asymmetric Notch activation specifies photoreceptors R3 and R4 and planar polarity in the *Drosophila* eye. *Nature* **397**, 523-526.

Fanto, M., Weber, U., Strutt, D. I. and Mlodzik, M. (2000). Nuclear signaling by Rac abd Rho GTPases is required in the establishment of epithelial planar polarity in the *Drosophila* eye. *Curr. Biol.* **10**, 979-988.

Feiguin, F., Hannus, M., Mlodzik, M. and Eaton, S. (2001). The Ankyrin repeat protein Diego mediates Frizzled-dependent planar polarization. *Dev. Cell* **1**, 93-101.

Gubb, D., Green, C., Huen, D., Coulson, D., Johnson, G., Tree, D., Collier, S. and Roote, J. (1999). The balance between isoforms of the prickle LIM domain protein is critical for planar polarity in Drosophila imaginal discs. *Genes Dev.* **13**, 2315-2327.

Jenny, A., Darken, R. S., Wilson, P. A. and Mlodzik, M. (2003). Prickle and Strabismus form a functional complex to generate a correct axis during planar cell polarity signaling. *EMBO J.* **22**, 4409-4420.

Keller, R. (2002). Shaping the vertebrate body plan by polarized embryonic cell movements. *Science* **298**, 1950-1954.

Lu, B., Usui, T., Uemura, T., Jan, L. and Jan, Y. N. (1999). Flamingo controls the planar polarity of sensory bristles and asymmetric division of sensory organ precursors in *Drosophila*. *Curr. Biol.* **9**, 1247-1250.

Ma, D., Yang, C. H., McNeill, H., Simon, M. A. and Axelrod, J. D. (2003). Fidelity in planar cell polarity signalling. *Nature* **421**, 543-547.

Mlodzik, M. (1999). Planar polarity in the *Drosophila* eye: a multifaceted view of signaling specificity and cross-talk. *EMBO J.* **18**, 6873-6879.

Mlodzik, M. (2002). Planar cell polarization: do the same mechanisms regulate Drosophila tissue polarity and vertebrate gastrulation? *Trends Genet.* **18**, 564-571.

Pignoni, F. and Zipursky, S. L. (1997). Induction of Drosophila eye development by decapentaplegic. *Development* **124**, 271-278.

Rawls, A. S. and Wolff, T. (2002). The cadherins fat and dachsous regulate dorsal/ventral signaling in the Drosophila eye. *Curr. Biol.* **12**, 1021-1026.

Rawls, A. S. and Wolff, T. (2003). Strabismus requires Flamingo and Prickle function to regulate tissue polarity in the Drosophila eye. *Development* **130**, 1877-1887.

Rorth, P. (1998). Gal4 in the Drosophila female germline. *Mech. Dev.* **78**, 113-118.

Spradling, A. C. and Rubin, G. M. (1982). Transposition of cloned P-elements into Drosophila germ line chromosomes. *Science* **218**, 341-347.
Strutt, D. I. (2001). Asymmetric localization of frizzled and the establishment of cell polarity in the Drosophila wing. *Mol. Cell* **7**, 367-375.
Strutt, D. (2003). Frizzled signalling and cell polarisation in Drosophila and vertebrates. *Development* **130**, 4501-4513.
Strutt, D., Johnson, R., Cooper, K. and Bray, S. (2002). Asymmetric localization of frizzled and the determination of notch-dependent cell fate in the Drosophila eye. *Curr. Biol.* **12**, 813-824.
Taylor, J., Abramova, N., Charlton, J. and Adler, P. N. (1998). Van Gogh: a new Drosophila tissue polarity gene. *Genetics* **150**, 199-210.
Tomlinson, A. and Struhl, G. (1999). Decoding vectorial information from a gradient: sequential roles of the receptors Frizzled and Notch in establishing planar polarity in the Drosophila eye. *Development* **126**, 5725-5738.
Tomlinson, A., Bowtell, D. D. L., Hafen, E. and Rubin, G. M. (1987). Localization of the *sevenless* protein, a putative receptor for positional information, in the eye imaginal disc of Drosophila. *Cell* **51**, 143-150.
Tree, D. R. P., Shulman, J. M., Rousset, R., Scott, M. P., Gubb, D. and Axelrod, J. D. (2002). Prickle mediates feedback amplification to generate asymmetric planar cell polarity signaling. *Cell* **109**, 371-381.
Uemura, T. and Shimada, Y. (2003). Breaking cellular symmetry along planar axes in Drosophila and vertebrates. *J. Biochem.* **134**, 625-630.
Usui, T., Shima, Y., Shimada, Y., Hirano, S., Burgess, R. W., Schwarz, T. L., Takeichi, M. and Uemura, T. (1999). Flamingo, a seven-pass transmembrane cadherin, regulates planar cell polarity under the control of Frizzled. *Cell* **98**, 585-595.
Veeman, M. T., Axelrod, J. D. and Moon, R. T. (2003). A second canon. Functions and mechanisms of beta-catenin-independent Wnt signaling. *Dev. Cell* **5**, 367-377.
Vinson, C. R. and Adler, P. N. (1987). Directional non-cell autonomy and the transmission of polarity information by the *frizzled* gene of *Drosophila*. *Nature* **329**, 549-551.
Wallingford, J. B., Rowning, B. A., Vogeli, K. M., Rothbacher, U., Fraser, S. E. and Harland, R. M. (2000). Dishevelled controls cell polarity during Xenopus gastrulation. *Nature* **405**, 81-85.
Wallingford, J. B., Fraser, S. E. and Harland, R. M. (2002). Convergent extension: the molecular control of polarized cell movement during embryonic development. *Dev. Cell* **2**, 695-706.
Wolff, T. and Ready, D. F. (1991). The beginning of pattern formation in the *Drosophila* compound eye: the morphogenetic furrow and the second mitotic wave. *Development* **113**, 841-850.
Wolff, T. and Ready, D. F. (1993). Pattern formation in the *Drosophila* retina. In *The development of Drosophila melanogaster* (ed. M. B. A. Martinez-Arias), pp. 1277-1326. Cold Spring Harbor, NY: Cold Spring Harbor Press.
Wolff, T. and Rubin, G. M. (1998). *strabismus*, a novel gene that regulates tissue polarity and cell fate decisions in *Drosophila*. *Development* **125**, 1149-1159.
Yang, C., Axelrod, J. D. and Simon, M. A. (2002). Regulation of Frizzled by fat-like cadherins during planar polarity signaling in the Drosophila compound eye. *Cell* **108**, 675-688.
Zeidler, M. P., Perrimon, N. and Strutt, D. I. (1999). The four-jointed gene is required in the Drosophila eye for ommatidial polarity specification. *Curr. Biol.* **9**, 1363-1372.
Zheng, L., Zhang, J. and Carthew, R. W. (1995). *frizzled* regulates mirror-symmetric pattern formation in the *Drosophila* eye. *Development* **121**, 3045-3055.